



Dielectric and Ferroelectric Properties of Ba(Zr_{0.35}Ti_{0.65})O₃ Thin Films Grown by a Sol-Gel Process

ZHAI JIWEI,^{1,*} YAO XI,¹ SHEN BO,¹ ZHANG LIANGYING¹ & HAYDN CHEN²

¹Functional Materials Research Laboratory, Tongji University, Shanghai 200092, People's Republic of China

²Department of Physics and Materials Science, City University of Hong Kong, Kowloon, Hong Kong

Submitted July 25, 2003; Revised December 23, 2003; Accepted January 19, 2004

Abstract. The Ba(Zr_{0.35}Ti_{0.65})O₃ (BZT) thin films were deposited via sol-gel process on LaNiO₃-coated silicon substrates. XRD showed that the crystallinity of BZT film grown on LaNiO₃ coated silicon substrates is better than that of BZT film grown on Pt. Both films showed perovskite phase and polycrystalline structure. The temperature dependent dielectric measurements revealed that the thin films had the relaxor behavior and diffuse phase transition characteristics. The capacitor tuning was about 44% for each BZT film grown on LaNiO₃/Pt and Pt electrodes at 1 MHz. Especially, the values of dielectric loss at 1 MHz ranged from ~0.02 to 0.009 in the bias range of 0 to 514 kV/cm, respectively. The leakage currents density of thin films grown on LaNiO₃/Pt and Pt electrodes at 300 kV/cm was about 8.5×10^{-7} and 1.1×10^{-5} A/cm², respectively. This work demonstrates a potential use of BZT films for application in tunable microwave devices.

Keywords: sol-gel, ferroelectric thin films, relaxor behavior, tunability

1. Introduction

For a larger number of lead-free BaTiO₃-based ceramics depending on the composition, some of them exhibit a relax behavior whose characteristics were related to the type of ionic substitutes and to substitution rate [1–4]. Zr is of interest because a different character of dielectric response with respect to the ferroelectric-to-paraelectric phase transition can be achieved by the substitution of Zr for Ti in BaTiO₃. The Zr⁴⁺ ion (atomic radius of 86 pm) is chemically more stable than the Ti⁴⁺ (atomic radius of 74.5 pm) and has a larger ionic size to expand the perovskite lattice. Therefore, barium zirconium titanate Ba(Zr_xTi_{1-x})O₃ (BZT) materials exhibits several interesting features in the dielectric behavior of BaTiO₃ materials. For the highest values of $x > 0.27$ there was only one broad peak in the dielectric constant at T_{\max} with frequency dispersion for $T \leq T_{\max}$ and an increase of T_{\max} when frequency increased, thus exhibiting typical relaxor-like

behavior. Lead-free composition in these materials could prove valuable for capacitors, actuators and dynamic random access memory application because they are environment-friendly.

In this paper, we reported the results of the investigation of microstructure and dielectric behavior of the BZT films grown on LaNiO₃ as a buffer layer on Pt/Ti/SiO₂/Si substrates. The electric properties of the BZT films were studied as a function of frequency, temperature and electric field.

2. Experimental Processing

The barium acetate [Ba(CH₃COO)₂], zirconium isopropoxide [Zr(OC₃H₇)₄], and titanium isopropoxide [Ti(OC₃H₇)₄] were used as starting materials. Acetic acid was used as a solvent. Ba(CH₃COO)₂ was heated and dissolved in acetic acid. After cooling to room temperature, Zr(OC₃H₇)₄ and Ti(OC₃H₇)₄ were added in the solution. Ethylene glycol [CH₂OHCH₂OH] was added to control the viscosity and cracking of films; the solution was mixed and refluxed for 1 h. The

*To whom all correspondence should be addressed. E-mail: zhajiwei@eastday.com

concentration of the final solution was adjusted to about 0.1 M. After aging the hydrolyzed solution for 24 h, thin-film deposition was carried out on the $\text{LaNiO}_3/\text{Pt}/\text{Ti}/\text{SiO}_2/\text{Si}(100)$ and $\text{Pt}/\text{Ti}/\text{SiO}_2/\text{Si}(100)$ substrates by spin coating at 3000 rpm for 30 s each layer.

The thickness of LaNiO_3 (LNO), Pt, Ti, and SiO_2 were 150, 150, 50, and 150 nm, respectively. The LNO layer was prepared by magnetron sputtering. Before spin coating of the BZT, the LNO covered substrates were annealed at 800°C for 30 min to promote grain growth. Each spin-coated BZT layer was subsequently heat treated at 500°C for 5 min. The coating and heat treatment procedures were repeated several times until reaching the desired thickness. The BZT films with the thickness of 350 nm were grown in this study.

The crystalline phase of the thin films was identified by X-ray diffraction (SIEMENS D-500 powder diffractometer). The film thickness and the surface morphology were determined by FESEM. For the electrical measurements, a top gold electrode of $400 \times 400 \mu\text{m}^2$ in square was deposited by DC-sputtering. The current-voltage (I-V) characteristics were measured by a HP 4140B. The capacitance-voltage (C-V) and capacitance-frequency (C-F) characteristics were measured using an Agilent 4284A LCR meter.

3. Results and Discussion

Figure 1 shows the XRD patterns for the BZT thin films. It is evident that the BZT films are polycrystalline and perovskite phase when deposited on the two kinds of substrates. At the same annealing temperature, the films deposited on the $\text{LaNiO}_3/\text{Pt}/\text{Ti}/\text{SiO}_2/\text{Si}(100)$ substrate tend to show better crystallinity. It was seen that when the films are deposited on the $\text{LaNiO}_3/\text{Pt}/\text{Ti}/\text{SiO}_2/\text{Si}(100)$ substrate, (100) and (200) peaks were similar in intensity to the (110) peak. For the films deposited on the $\text{Pt}/\text{Ti}/\text{SiO}_2/\text{Si}(100)$ substrates, the (100) and (200) peaks are nearly absent. The growth behavior and orientation of crystallites can be influenced by several factors: lattice match or mismatch with substrate, regular defects on the surface of the substrate, surface and interfacial energies, etc. The (100) orientation of the LaNiO_3 layer and the good match of the lattice constants between LaNiO_3 and BZT could be the reasonable interpretations for the enhanced (100) and (200) BZT peaks.

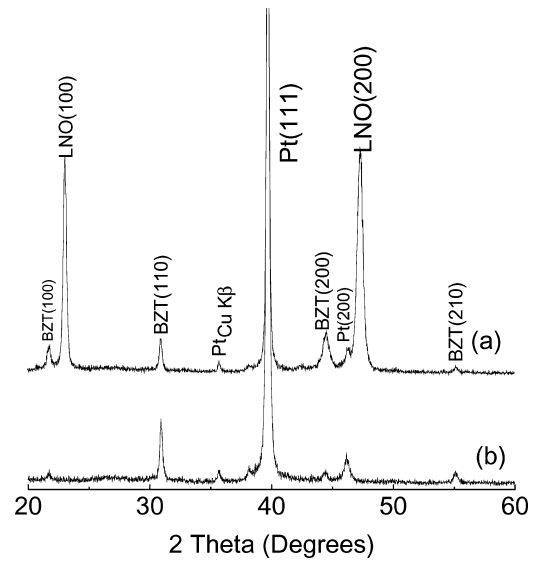


Fig. 1. XRD patterns of sol-gel deposited $\text{BaZr}_{0.35}\text{Ti}_{0.65}\text{O}_3$ thin films on (a) $\text{LaNiO}_3/\text{Pt}/\text{Ti}/\text{SiO}_2/\text{Si}(100)$ and (b) $\text{Pt}/\text{Ti}/\text{SiO}_2/\text{Si}(100)$ substrates.

Figure 2 shows SEM images of the sol-gel deposited $\text{BaZr}_{0.35}\text{Ti}_{0.65}\text{O}_3$ thin films on (a) $\text{LaNiO}_3/\text{Pt}/\text{Ti}/\text{SiO}_2/\text{Si}(100)$, (b) $\text{Pt}/\text{Ti}/\text{SiO}_2/\text{Si}(100)$ substrates, (c) cross sectional morphology of (a) and (d) cross sectional morphology of (b). As shown in Fig. 2, BZT thin films deposited on the $\text{Pt}/\text{Ti}/\text{SiO}_2/\text{Si}(100)$ substrate have a grain size smaller than 30 nm. The morphologies of the BZT thin film deposited on the $\text{LNO}/\text{Pt}/\text{Ti}/\text{SiO}_2/\text{Si}(100)$ substrate shown in Fig. 2(a) show grain size of 30–50 nm. Compared with the thin films deposited on $\text{Pt}/\text{Ti}/\text{SiO}_2/\text{Si}$ substrate, the BZT thin films could be crystallized at lower temperature as deposited on the LNO-buffer $\text{Pt}/\text{Ti}/\text{SiO}_2/\text{Si}$ substrates [5]. Therefore, crystallization may start at lower temperature, resulting in a larger grain size for the same heat treatment conditions.

The dielectric constant and dielectric loss of BZT thin films as a function of temperature is shown in Fig. 3. One broad peak was obviously observed in the dielectric constant at transition temperature (T_{max} , denoted by the peak temperature of the dielectric constant maxima) with frequency dispersion for $T = T_{\text{max}}$, the position of T_{max} slightly increased as the frequency increased. The temperature dependent dielectric constant is significantly different from that of the bulk material. The dielectric constant versus temperature curves for the films is much broader than that of the bulk ceramics. The phase transition was diffused in nature, which

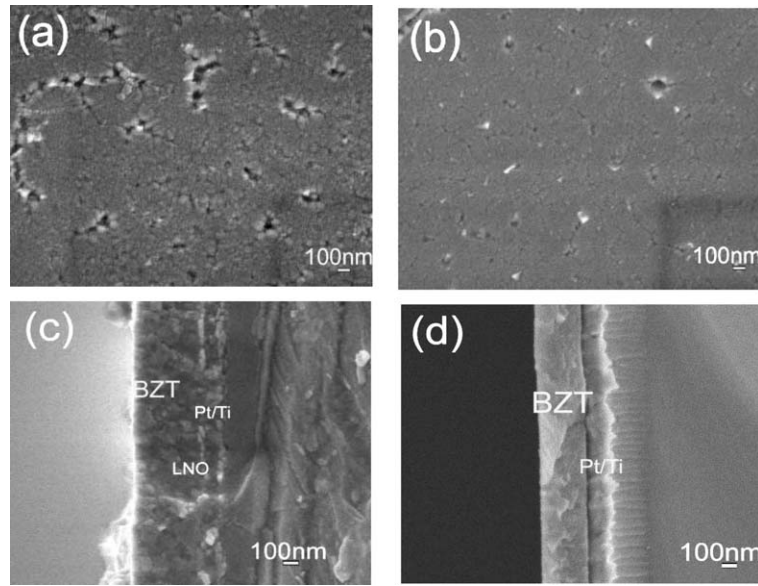


Fig. 2. SEM micrographs of sol-gel deposited $\text{BaZr}_{0.35}\text{Ti}_{0.65}\text{O}_3$ thin films on (a) $\text{LaNiO}_3/\text{Pt}/\text{Ti}/\text{SiO}_2/\text{Si}(100)$ and (b) $\text{Pt}/\text{Ti}/\text{SiO}_2/\text{Si}(100)$ substrates, (c) cross sectional morphology of (a), and (d) cross sectional morphology of (b).

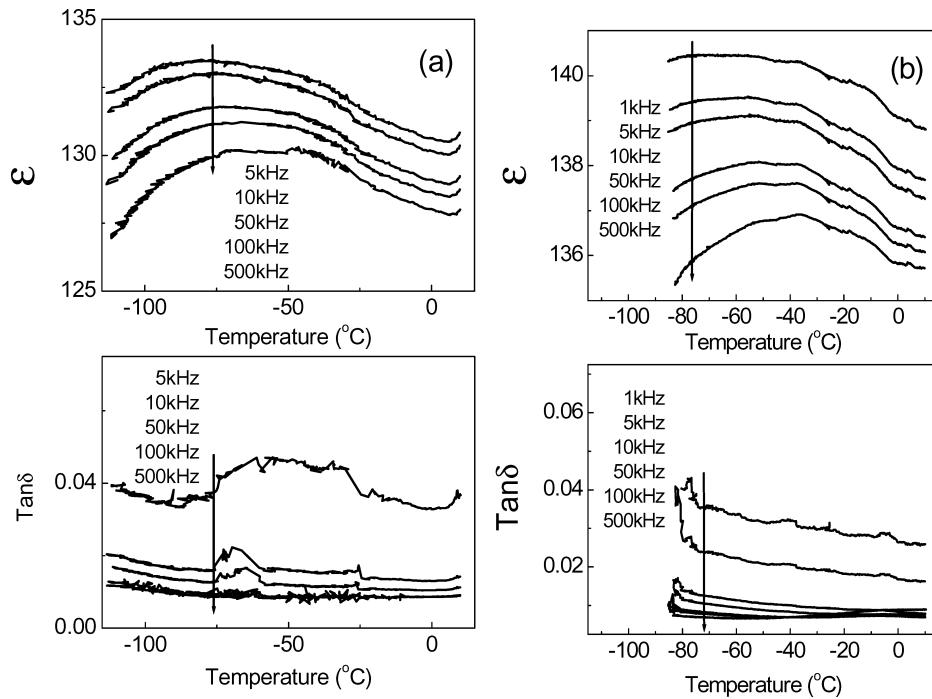


Fig. 3. The dielectric constant and dielectric loss of BZT thin film deposition on (a) $\text{LaNiO}_3/\text{Pt}/\text{Ti}/\text{SiO}_2/\text{Si}(100)$ and (b) $\text{Pt}/\text{Ti}/\text{SiO}_2/\text{Si}(100)$ substrates as a function of temperature.

occurred between -100°C and -20°C . The transition temperature of BZT films grown on LaNiO_3/Pt and Pt electrodes is about -66°C and -45°C at 100 kHz, respectively. The transition temperature of BZT films grown on Pt electrode is obviously higher than the bulk transition temperature (-63°C at 100 kHz [2]). Similar phenomenon was reported in BST and BZT thin film [6, 7]. The shifts of transition temperature in films could be attributed to the strain accumulated within the BZT films. Films strain can originate from several sources including the deposition process, lattice mismatch, and thermal expansion mismatch between substrate and thin film. The broadening of transition temperature in thin films was due to the fine grained structure [8] and unrelaxed growth strain [6, 9]. As shown in Fig. 3(b), the peaks of dielectric loss were not observed in BZT films grown on Pt/Ti/SiO₂/Si(100) substrate due to fine grain size.

Figure 4 shows the dielectric constant as a function of applied DC bias field for BZT thin films at room temperature and the frequency range of 1–1000 kHz. The results were similar to that of BST material [10]. The dielectric constant of BZT thin films deposited on LaNiO_3/Pt and Pt electrodes showed DC bias de-

pendent dielectric constant behaviors. At the applied electric field of 514 kV/cm, tuning of BZT films grown on LaNiO_3/Pt and Pt electrodes were about 44%. The dielectric loss of BZT films grown on LaNiO_3/Pt and Pt electrodes at 1 MHz ranged from ~ 0.02 to 0.009 in the bias range of 0 to 514 kV/cm (18 V), respectively. The loss tangent measurements as a function of bias voltage showed similar behaviors with that of tuning curves.

The difference in the leakage current characteristics of BZT thin film shown in Fig. 5 indicates the change of current density J versus applied DC electric field E of the films measured at room temperature. It is seen that the leakage current density of the BZT thin film deposited on the $\text{LaNiO}_3/\text{Pt}/\text{Ti}/\text{SiO}_2/\text{Si}(100)$ substrates is about 1 order of magnitude lower than that for the BZT thin film deposited on the Pt/Ti/SiO₂/Si(100) substrates. The current density increases linearly with the applied DC electric field in the range of higher electric field up to 420 kV/cm. It is generally known that the leakage often abruptly turns up in orders of magnitude as the applied voltage exceeds a critical field of several hundreds kV/cm, and there was a nonlinearity observed in the range of high electric field [11]. The leakage currents density of thin films grown on

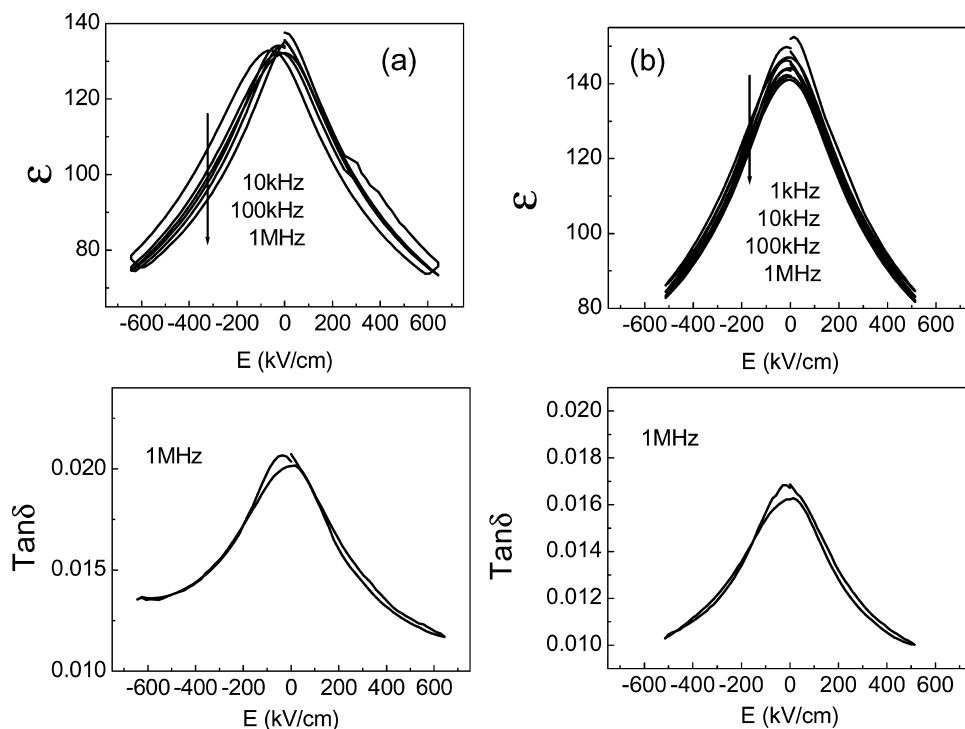


Fig. 4. ϵ - E characteristics of BZT thin films deposition on (a) $\text{LaNiO}_3/\text{Pt}/\text{Ti}/\text{SiO}_2/\text{Si}(100)$ and (b) Pt/Ti/SiO₂/Si(100) substrates.

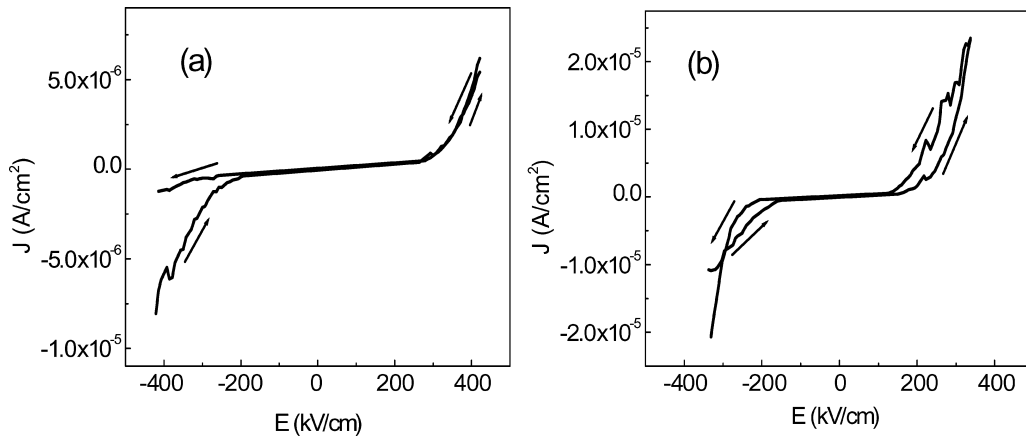


Fig. 5. J-E characteristics of BZT thin films deposition on (a) LaNiO₃/Pt/Ti/SiO₂/Si(100) and (b) Pt/Ti/SiO₂/Si(100) substrates.

LaNiO₃/Pt and Pt electrodes at 300 kV/cm was about 8.5×10^{-7} and 1.1×10^{-5} A/cm², respectively. In the BZT thin films, the low and stable leakage current was maintained. This is possible because the substitution of Ti with Zr would depress the conduction by electronic hopping between Ti⁴⁺ and Ti³⁺, and it would also decrease the leakage current of the BaTiO₃ thin film system.

The leakage current characteristics are also different in the positive and negative voltage region. The different of reverse currents might be caused by the different top electrode (Au/BZT) and bottom electrode (LNO/BZT or Pt/BZT) work functions in the two interfaces. It implies that the leakage current is electrode limited [12, 13]. Therefore, if these potential barriers were identical at the interfaces of electrode and films, then the *J*-*E* characteristics would be symmetric.

4. Conclusion

The BaZr_{0.35}Ti_{0.65}O₃ thin films were prepared on LaNiO₃/Pt and Pt electrodes substrates by sol-gel methods. The films were single perovskite phase. From the temperature dependent dielectric measurements, one can conclude that the thin films have the relaxor behavior and diffuse phase transition characteristics. The capacitor tuning was about 44% for each BZT film grown on LaNiO₃/Pt and Pt electrodes at 1 MHz. Especially, the values of dielectric loss at 1 MHz ranged from ~0.02 to 0.009 in the bias range of 0 to 514 kV/cm, respectively. The low and stable leakage current was maintained in the range of higher electric field. This work clearly reveals the

highly promising potential of BZT to replace BST films for application in tunable microwave devices.

Acknowledgments

This research was supported by the Ministry of Sciences and Technology of China through 973-project under grant 2002CB613304. This work was also supported by the university key studies project of Shanghai.

References

1. T.B. Wu, C.M. Wu, and M.L. Chen, *Appl. Phys. Lett.*, **69**, 2659 (1996).
2. J. Ravez and A. Simon, *Eur. Phys. J. AP*, **11**, 9 (2000).
3. A. Dixit, S.B. Majumder, A. Savvinov, R.S. Katiyar, R. Guo, and A.S. Bhalla, *Materials Letters*, **56**, 933 (2002).
4. Won Seok Choi, Bum Sik Jang, Dong-Gun lim, Junsin Yi, and Byungyou Hong, *Journal of Crystal Growth*, **237-239**, 438 (2002).
5. Jiwei Zhai and Haydn Chen, *Appl. Phys. Lett.*, **82**, 442 (2002).
6. C.M. Carlson, T.V. Rivkin, P.A. Parilla, J.D. Perkins, and D.S. Ginley, *Appl. Phys. Lett.*, **76**, 1920 (2000).
7. Nobuo Kamehara, Mineharu Tsukada, J.S. Cross, and Kazuaki Kurihara, *Ceramics Processing*, **43**(11A), 2844 (1997).
8. M.P. McNeal, S.C. Sun, and T.Y. Tseng, *J. Appl. Phys.*, **83**, 3288 (1998).
9. S. Bhaskar, S.B. Majumder, and R.S. Katiyar, *Appl. Phys. Lett.*, **80**, 3997 (2002).
10. Jaemo Im, O. Auciello, P.K. Baumann, S.K. Streiffer, D.Y. Kaufman, and A.R. Krauss, *Appl. Phys. Lett.*, **76**, 625 (2000).
11. S.B. Rupanidhi and C.J. Peng, *Thin Solid Films*, **305**, 144 (1997).
12. S.Y. Lee and T.Y. Tseng, *Appl. Phys. Lett.*, **80**, 1797 (2002).
13. K. Abe and S. Komatsu, *J. Appl. Phys.*, **77**, 6461 (1995).